Temporal dynamics of animacy categorization in the brain of patients with mild cognitive impairment

Hamed Karimi[1,2,*], Haniye Marefat[3], Mahdiyeh Khanbagi[2], Chris Kalafatis[4,5,6], Hadi Modarres[6], Zahra Vahabi[7,8], Seyed-Mahdi Khaligh-Razavi[2,6,*]

[1]Department of Mathematics and Computer Science, Amirkabir University of Technology, Tehran, Iran

[2]Royan Institute for Stem Cell Biology and Technology, ACECR, Tehran, Iran

[3]School of Cognitive Sciences, Institute for Research in Fundamental Sciences (IPM), Tehran, Iran

[4]South London & Maudsley NHS Foundation Trust, London, UK

[5]Department of Old Age Psychiatry, King's College London, London, UK

[6]Cognetivity ltd, London, UK

[7]Department of Geriatric Medicine, Ziaeian Hospital, Tehran University of Medical Sciences, Tehran, Iran

[8]Memory and Behavioral Neurology Division, Roozbeh Hospital, Tehran University of Medical Sciences, Tehran, Iran

*Corresponding authors:

Hamed Karimi
(hamedk72@gmail.com)

Seyed-Mahdi Khaligh Razavi
(seyed@cognetivity.com)

Keywords: Electroencephalography, Mild Cognitive Impairment, Multivariate Pattern Analysis

Abstract

Electroencephalography (EEG) has been commonly used to measure brain alterations in Alzheimer's Disease (AD). However, reported changes are limited to those obtained from using univariate measures, including activation level and frequency bands. To look beyond the activation level, we used multivariate pattern analysis (MVPA) to elicit the pattern of information processing from EEG responses to an animacy categorization task. Comparing healthy controls (HC) with patients with mild cognitive impairment (MCI), we found that the neural speed of animacy information processing is decreased in MCI patients. Moreover, we found critical time-points during which the representational pattern of animacy for MCI patients was significantly discriminable from that of HC, while the activation level remained unchanged. Together, these results suggest that the speed and pattern of animacy information processing provide clinically useful information as a potential biomarker for detecting early changes in MCI and AD patients.

Introduction

Mild Cognitive Impairment (MCI) is a condition in which an individual has a mild but measurable decline in cognitive abilities. This decline is noticeable to the person affected and to the family members and friends, but the individual can still carry out everyday activities ("2018 Alzheimer's Disease Facts and Figures" 2018). A systematic review of 32 cohort studies shows an average of 32 percent conversion from MCI to Alzheimer's Disease (AD) within a five-year follow-up (Ward et al. 2013).

Electroencephalography (EEG) is widely used to study the resting-state neural activity in the brain of patients with MCI and mild AD (Vecchio et al. 2014; Babiloni et al. 2016; Pijnenburg et al. 2004; Moretti et al. 2011; Poil et al. 2013; Babiloni et al. 2017; Vecchio et al. 2017). A few studies have also used EEG to associate abnormalities in memory function with cognitive impairment during both encoding and decoding stages of working memory (Pijnenburg et al. 2004; P. Missonnier et al. 2007; Francisco J. Fraga et al. 2018; F. J. Fraga et al. 2017) as well as episodic memory tasks (Han et al. 2017).

The relationship between cognitive impairment and visual system changes has recently gained attention (Paik et al. 2020). Several studies have linked deficiencies in different parts of the visual system with AD (D. G. Cogan 1979; Jackson and Owsley 2003). There are several documented cases in which visual function problems are the initial and dominant manifestation of progressive dementia (Sadun et al. 1987; David G. Cogan 1985). A few studies have also used a visual task to report changes in the EEG responses of patients with MCI and AD (van Deursen et al. 2008; Briels et al. 2020).

Several studies of the visual system in primates and healthy human subjects have demonstrated that images are categorized by their animacy status (i.e. animate vs. inanimate) in the higher-level visual areas (Kiani et al. 2007; Kriegeskorte et al. 2008; Connolly et al. 2012; Khaligh-Razavi and Kriegeskorte 2014; Khaligh-Razavi et al. 2017; Naselaris, Stansbury, and Gallant 2012). The neural activity underlying the animacy information processing of briefly flashed images was also studied in healthy adults (Bacon-Macé et al. 2005; Thorpe 2009). Studies have shown that animacy information emerges in the brain of healthy human subjects as early as 80 ±20 ms after the stimulus onset and reaches its peak within 250 ±50ms after the stimulus onset (Cichy, Pantazis, and Oliva 2014; Carlson et al. 2013; Khaligh-Razavi et al. 2018). However, the underlying neural dynamics of animacy processing in the brain of patients with MCI in comparison to healthy controls (HC) is still unknown.

The Integrated Cognitive Assessment (ICA) is a visual task based on a rapid categorization of natural images of animals and non-animals (Khaligh-Razavi et al. 2019). ICA assesses changes in the speed and accuracy of animacy processing in patients with

MCI and mild AD, and is shown to be sensitive in detecting MCI patients (Kalafatis and Khaligh Razavi 2019; Kalafatis et al. 2019).

Here we acquired EEG data from MCI and HC participants while they were doing the ICA's animal/non-animal categorization task. We studied the temporal neural dynamics of animacy processing in MCI patients using both univariate and multivariate analyses. By applying multivariate pattern analysis (MVPA), we compared the neural speed of animacy processing in MCI and healthy individuals. We further looked beyond the conventional univariate methods and compared MCI and HC in terms of their pattern of EEG responses to natural images of animal and non-animal stimuli.

We find that the categorical representation of animacy information emerges later in the brain of patients with MCI compared to that of HC. Furthermore, the results reveal differences between the EEG response patterns of HC vs. MCI during the time-points when univariate mean responses showed no significant difference. The EEG response patterns could further be used to discriminate HC from MCI, demonstrating that the pattern of EEG activity also carries information about the status of the disease, beyond the conventional univariate analysis of mean activities.

Methods

Integrated Cognitive Assessment (ICA) Task

ICA (Khaligh-Razavi et al. 2019) is a rapid animal vs. non-animal categorization task. The subjects are presented with natural images of animals and non-animals. The images are followed by a short blank screen and then a dynamic mask. Subjects should categorize the images as animal or non-animal as quickly and accurately as possible (Figure 1). See (Khaligh-Razavi et al. 2019, Figure 1B) for sample images of the task.

Montreal cognitive assessment (MoCA)

MoCA (Nasreddine et al. 2005) is a ten-minute pen and paper test with a maximum score of 30 and is conventionally used to assess visuospatial, memory, attention, and language abilities to detect cognitive impairment in older adults. An examiner is needed to administer the test.

Addenbrooke Cognitive Examination (ACE-R)

ACE-R (Mioshi et al. 2006) is another pen-and-paper tool for cognitive assessment with a maximum score of 100. It mainly assesses five cognitive domains: attention, orientation,

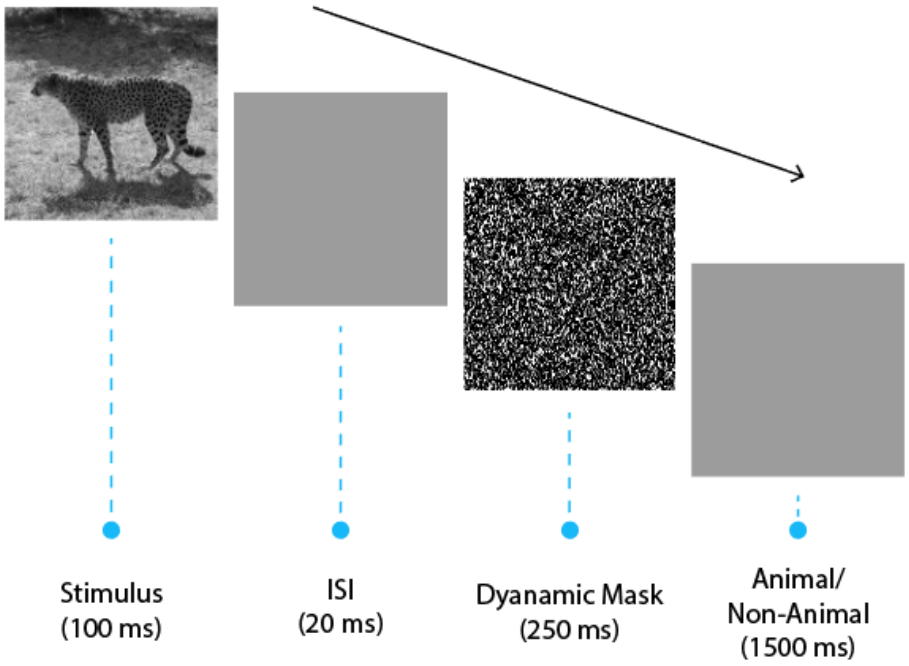

Figure 1. The EEG task. The EEG experiment contained 13 experimental runs; in each run, 32 natural images (16 animal, 16 non-animal) were presented to the subject in random order. Each image was shown for 100 ms, followed by an inter-stimulus interval (ISI) of 20ms and a dynamic noise mask for 250ms. Subjects were given 1500 ms to indicate (using pre-specified buttons) whether the presented image contained an animal or not.

memory, fluency, language, and visuospatial. On average, the test takes about 20 to 30 minutes to administer and score.

Subject Recruitment

40 (22 Healthy, 18 MCI) participants (Table 1) completed the ICA test, MoCA, and ACE-R in the first assessment. The participants were non-English speakers, with instructions for the cognitive assessments provided in Farsi. The ICA test was administered on an iPad.

Patients were recruited into the study prospectively. A consultant neurologist made all the diagnoses according to diagnostic criteria described by the working group formed by the National Institute of Neurological and Communicative Disorders and Stroke (NINCDS) and the Alzheimer's Disease and Related Disorders Association (ADRDA) (referred to as the NINCDS-ADRDA criteria) and the National Institute on Aging and Alzheimer's Association (NIA-AA) diagnostic guidelines. The study was conducted at the Royan Institute, according to the Declaration of Helsinki and approved by the local ethics committee at the Institute. The inclusion/exclusion criteria are listed below in more detail.

Table 1. Demographic information of participants
SD: standard deviation
p-values were calculated from two-sided t-test for two independent samples

Characteristic	HC (*n = 22*)	MCI (*n = 18*)	*P-values*
Age –mean years ±SD	63.23 ±6.18	63.55 ±6.40	0.87
Education in years –mean ±SD	15 ±4.18	14.72 ±5.02	0.85
Gender (%female)	13 (59%)	10 (55%)	0.82

- Inclusion criteria for the control group:

  Males and females aged between 50-85 years who are not currently on medication that may interfere with the study results and are in good general health were included in the study.

- Inclusion criteria for the MCI group:

  Males and females aged between 50-85 years with a clinical diagnosis of MCI who were able to provide informed consent were included in the study.

- Exclusion criteria for both groups:

  Individuals with a presence of significant cerebrovascular disease or major psychiatric disorder (e.g., Chronic psychosis, recurrent depressive disorder, generalized anxiety disorder, and bipolar mood disorder) or major medical comorbidities (e.g., Congestive Cardiac Failure, Diabetes Mellitus with renal impairment) were excluded from the study.

  Additional exclusion criteria were: use of cognitive-enhancing drugs (e.g., cholinesterase inhibitors)**,** or a concurrent diagnosis of epilepsy or any history of alcohol misuse**,** illicit drug abuse**,** severe visual impairment (e.g., macular degeneration, diabetic retinopathy, as determined by the clinical examination)**,** or repeated head trauma.

EEG Data Acquisition and Preprocessing

The EEG experiment included a short version of the ICA task. Participants completed one EEG session that included 13 runs; each run lasted 67 seconds, during which 32 images

were presented in random order, and participants had a short break in between the runs. In other words, each stimulus is repeated 13 times during the whole EEG session (once in each run). These are referred to as repetition trials throughout the manuscript. Subjects 16 and 17 completed 10 runs, and subjects 12 and 22 completed 12 runs. We acquired the EEG data using a 64 channel (63 electrodes on the cap and one as the reference) g.tec product at a sampling rate of 1200 Hz. Three electrooculograms (EOG) channels were set up to capture eye blinks.

The preprocessing consisted of six general steps: First, re-referencing the data with the mean activation and removing the reference channel (channel 33). Second, neutralizing eye blinks by removing the most correlated component with the EOG channels, using the independent component analysis algorithm. Third, extracting pre-stimulus data from 100ms before to 800 ms after the stimulus onset (epoching). Fourth, normalizing the epochs with regard to the mean and standard deviation of the baseline. Fifth, smoothing the data with a 50 Hz low-pass filter, and finally, sixth, resampling the data to 1000 Hz sampling rate. We have done all the preprocessing procedures using Brainstorm (Tadel et al. 2011) in MATLAB.

Univariate Pattern Analysis - Event-Related Potential (ERP)

We calculated the ERPs of the extracted epochs (from 100ms before to 800 ms after the stimulus onset) by averaging the EEG responses to all stimuli within each group of channels. We calculated the ERPs separately for each individual. The ERP of HC and MCI are the average ERP of corresponding subjects.

Multivariate Pattern Analysis - Animal vs. non-Animal Decoding

To study the emergence of animacy categorical information in the brain, we used a linear classifier to discriminate EEG responses to animal stimuli from that of non-animal (Figure 2). Before the classification, we randomly assigned each target stimulus with all its EEG trials to bins of size 2, 3, and 4 stimuli and randomly sub-averaged the trials within each bin. The decoding accuracy at each time-point ‘t’ is then the average accuracy of 10,000 repetitions in a leave-one-bin-out cross-validation model, using a support vector machine (SVM) classifier. The classification is done using the LIBSVM software implementation (Chang and Lin 2011).

Multivariate Pattern Analysis - Pairwise Decoding

At each time-point, we measured the accuracy of an SVM classifier in discriminating pairs of stimuli using leave-one-out cross-validation. This leads to a symmetric 32×32 representational dissimilarity matrix (RDM) at each time-point, representing the pairwise

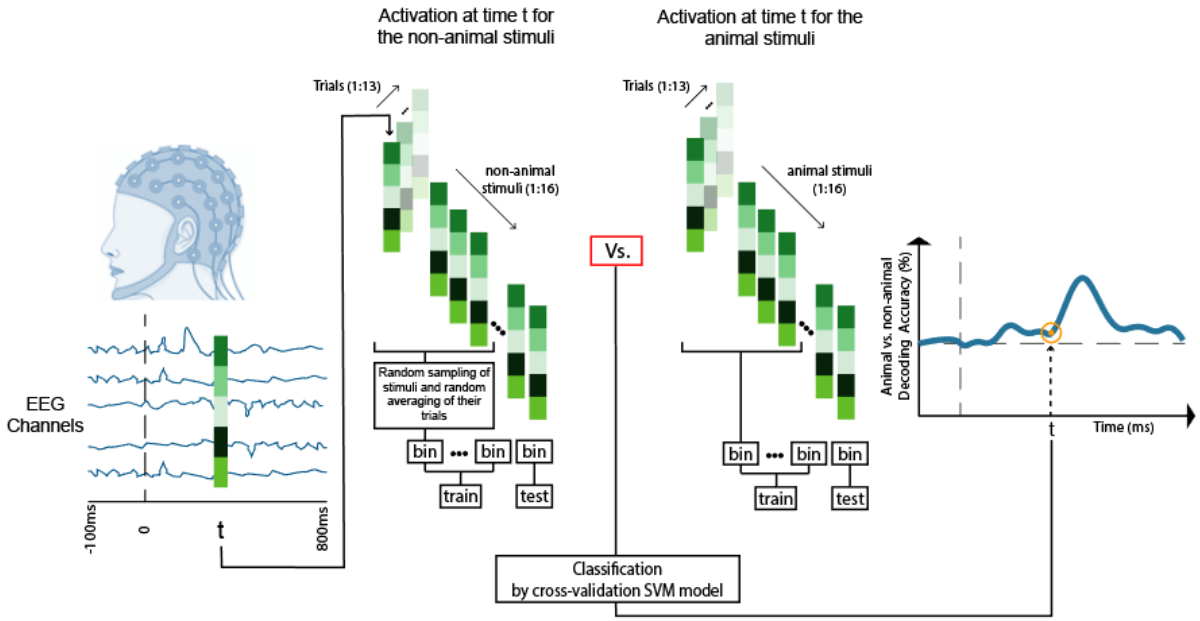

Figure 2. Animal vs. non-animal decoding. For each individual, we extracted the trials of EEG responses to animal and non-animal stimuli at each time-point (for a given time-point t we have two matrices of 63 channels x16 stimuli x13 repetition trials for animal and non-animal stimuli, respectively). Before the classification, we randomly assigned each target stimulus with all its EEG trials to bins of size 2, 3 and 4 stimuli and randomly sub-averaged the trials within each bin. We trained a leave-one-bin-out cross-validation SVM model to discriminate animal from non-animal. At each time-point, the decoding accuracy is the average of 10,000 repetitions of the classification procedure described above.

dissimilarities of stimuli in the off-diagonal elements (Figure 3). We repeated the entire process for each individual to create an RDM at each time-point.

Multivariate Pattern Analysis - HC vs. MCI Classification

We characterized the activations pattern at each time-point as a 63×32 matrix, with each row being the responses of the EEG channels to a stimulus, averaged over all repetition trials (Figure 4). We applied 10,000 bootstrap resamplings (without replacement) of participants and trained a leave-one-out cross-validation SVM model to discriminate the EEG activation pattern of HC from that of MCI.

Multidimensional Scaling (MDS)

Multidimensional Scaling (MDS) is a non-linear dimension reduction algorithm. It rearranges the data point in a p-dimensional space until the pairwise distance is consistent with a given dissimilarity matrix. Here, we used MDS to visualize the stimuli on a 2D plane based on their pairwise dissimilarity in RDMs.

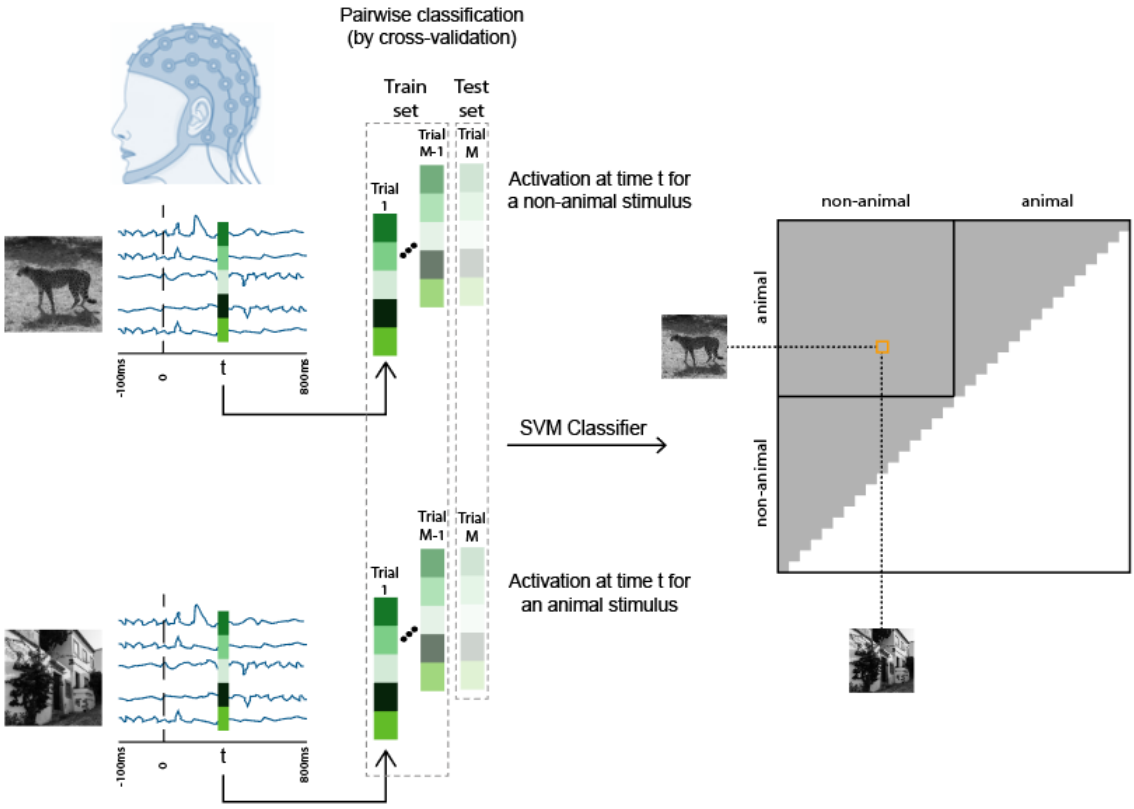

Figure 3. Representational dissimilarity matrices (RDMs). We trained an SVM to discriminate pairs of stimuli using their EEG responses at time-point t. This pairwise classification of stimuli by cross-validation SVM model leads to a 32 × 32 RDM at each time-point t.

Statistical Significance

To avoid any assumption about the observed distributions, we only used non-parametric statistical tests. They are capable of testing a null hypothesis without any prior assumptions about the nature of the distribution:

a) Bootstrap Test

Bootstrapping is a strategy to estimate different statistics over an unknown distribution. It consists of a resampling (with or without replacement) procedure and applying a target function. The result is a bootstrap distribution that can be used for statistical inference purposes. We used 10,000 bootstrap resampling of participants without replacement from each group (HC and MCI) and computed a p-value as follows:

$$p - value = \frac{number\ of\ elements\ lower\ (or\ higher)\ than\ baseline + 1}{number\ of\ bootstrap\ resampling\ (10000) + 1}$$

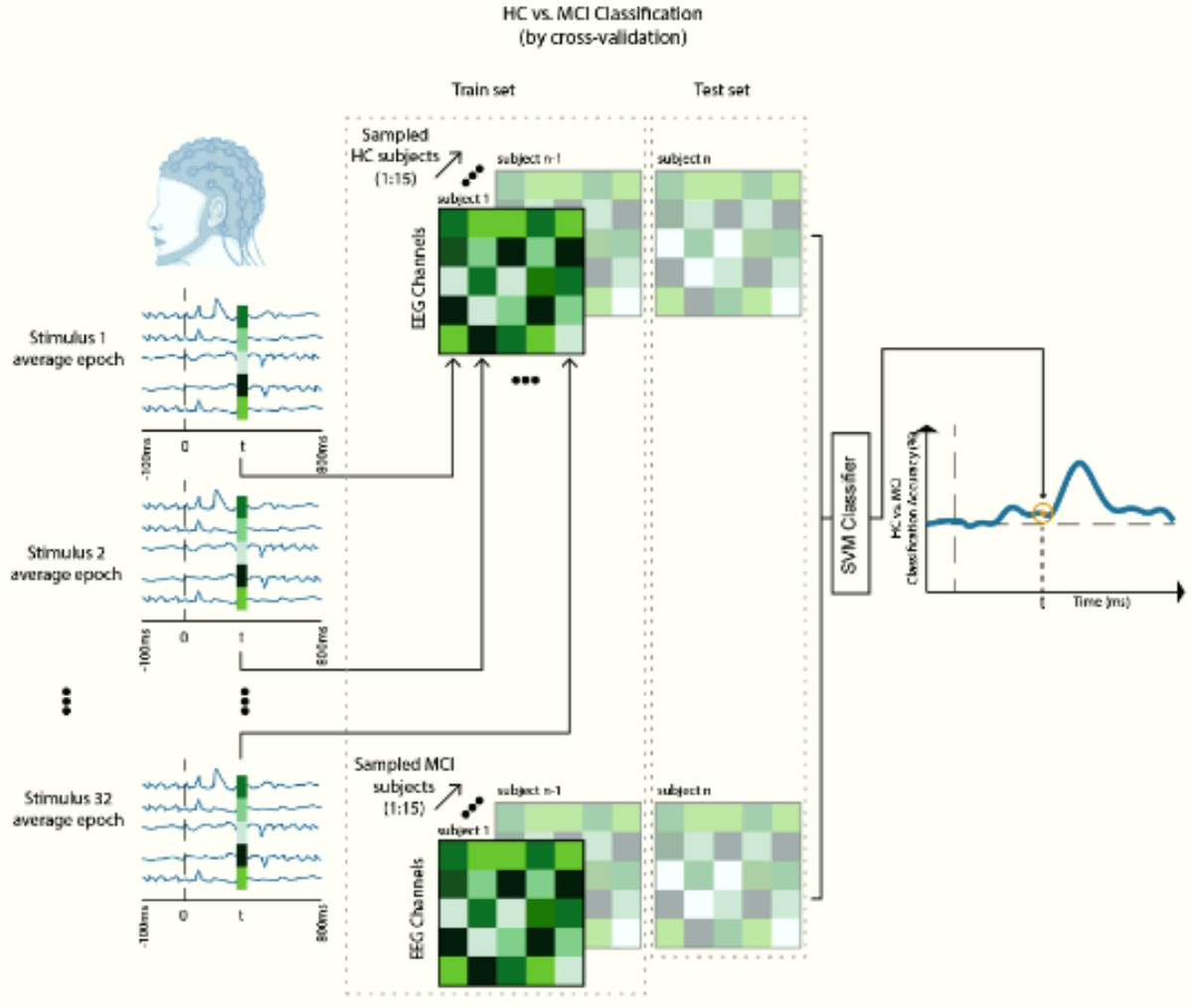

Figure 4. HC vs. MCI classification over time based on EEG response patterns. At each time-point, the pattern of EEG activation is a 63x32 matrix with columns being the EEG responses of channels to the 32 stimuli. We applied 10000 bootstrap resamplings (without replacement) of participants and each time trained a leave-one-out cross-validation SVM model to discriminate HC from MCI based on their EEG activation patterns.

b) *Permutation Test*

Permutation test consists of randomly relabeling the samples from two populations to form a null distribution. It computes a p-value by testing a target statistic against the null hypothesis:

$$p - value = \frac{number\ of\ members\ from\ the\ null\ distibution\ lower\ (or\ higher)\ than\ the\ target + 1}{number\ of\ permutations\ (10000) + 1}$$

c) *Rank-Sum*

Rank-sum (also known as Wilcoxon–Mann–Whitney test) tests the null hypothesis that the data in *x* and *y* are sampled from continuous distributions with equal medians,

against the alternative that they are not (*Nonparametric Statistical Inference* 2010). We used rank-sum to compute the p-value when comparing HC and MCI medians of animal vs. non-animal decoding amplitude, ICA speed and accuracy and, mean of ERP responses.

Result

A decrease in the speed and accuracy of animacy processing in MCI patients

We compared the neural speed and accuracy of animal/non-animal discrimination between healthy and MCI. To this end, for each group, we computed the time at which animal images can best be discriminated from non-animals based on their EEG responses. This time-point is referred to as the peak of animal/non-animal decoding. MCI patients show a delay of 39ms (95% CI= [8, 111], SE = 34 ms) in processing the animacy information in comparison to healthy individuals (p-value = 0.0001; 10000 bootstrap resampling of participants, Figure 5a)**.** Additionally, in this decoding peak time-point, the neural accuracy of animal detection is significantly lower in MCI patients compared to healthy controls (HC) (p-value = 0.018; rank-sum, Figure 5b).

The representational dissimilarity method is a way to represent patterns of brain information processing (Kriegeskorte and Kievit 2013). To study the neural representation underlying animacy categorization, we compared the representational dissimilarity matrices (RDM) and ERP responses (Figures 5c, 5d) of the two groups at the time of each individual's animal vs. non-animal decoding peak.

The HC/MCI RDM in the peak animacy decoding time-point represents the pattern of EEG responses at a time-point in which the brain representation of animal images is best separated from that of non-animals (Figure 5c**)**. While the peak animacy time-point was delayed for the MCI group, the MCI RDM was not significantly different from that of the HC RDM in its peak, suggesting that it took more time for the MCI patients to converge to a pattern similar to that of the HC, which is used for discriminating animals from non-animals.

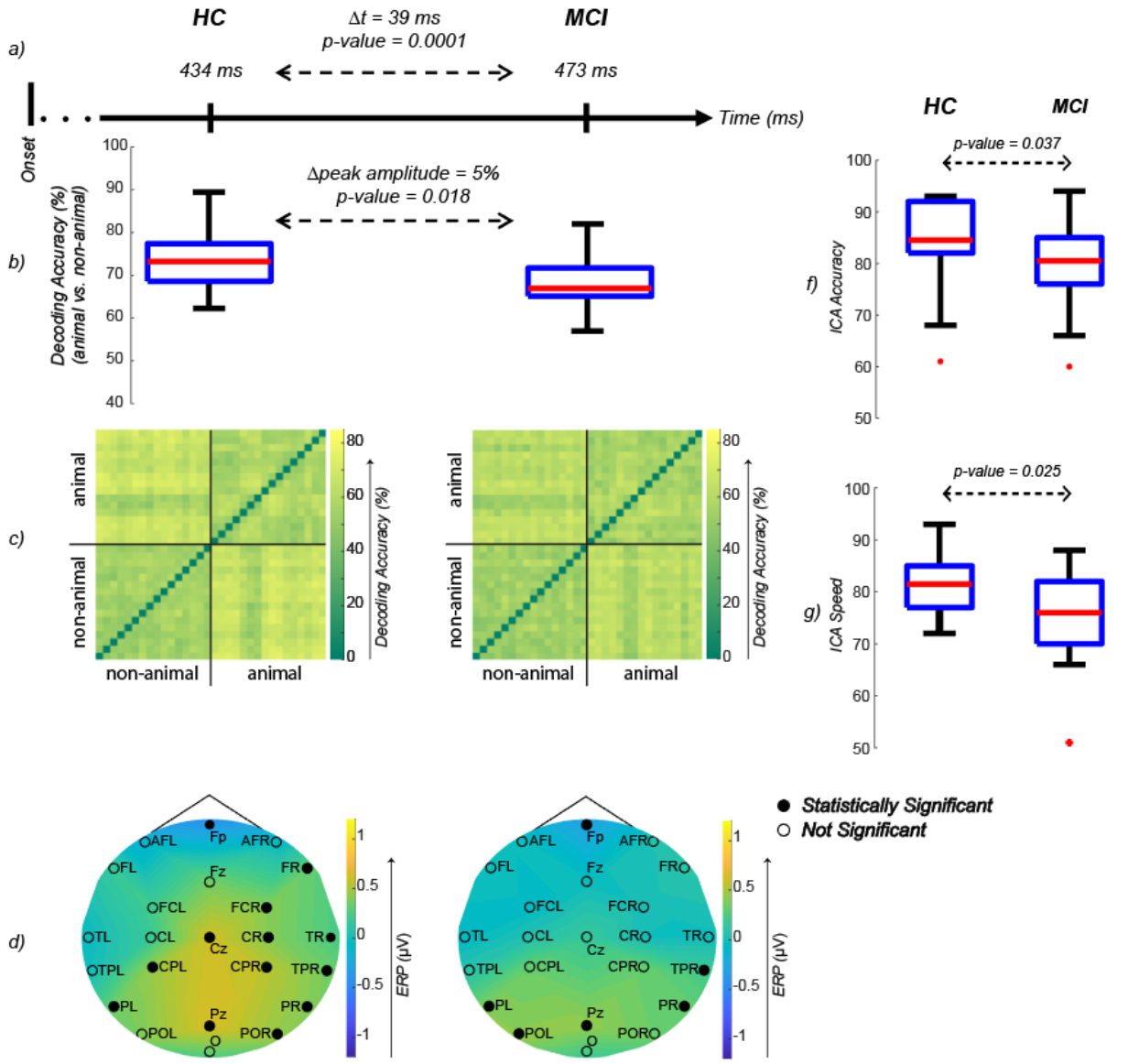

Figure 5. ***a)*** *Median of animal vs. non-animal decoding accuracy peak time-points. 10000 bootstrap resampling without replacement of participants was applied to measure the differences between HC and MCI. The median of time differences between MCI and HC is 39ms (p-value = 0.0001; One-sided bootstrap test)* ***b)*** *Box-plot of animal vs. non-animal EEG decoding peak amplitude. The difference of HC and MCI amplitude medians is 5% (p-value=0.018; rank-sum).* ***c)*** *Mean EEG RDM of subjects at the time of animal vs. non-animal decoding peak. No significant difference was observed between the RDMs (permutation test).* ***d)*** *Mean ERP of subjects at the time of animal vs. non-animal decoding peak. The black dots indicate significant activation in channels of the specified region (FDR-corrected at 0.05 sign-rank). No significant difference between the ERP of HC and MCI was observed (FDR-Corrected at 0.05 rank-sum).* ***f)*** *Box-plot of the ICA test accuracy (results of the behavioral ICA, taken on iPad). A significant difference is observed between HC and MCI (p-value = 0.037; rank-sum).* ***e)*** *Box-plot of the ICA test speed (results of the behavioral ICA, taken on iPad). A significant difference is observed between HC and MCI (p-value = 0.025; rank-sum).*

Fp: prefrontal; AFL: left anterior frontal; AFR: right anterior frontal; FL left frontal; Fz: midline frontal; FR: right frontal; FCL: left fronto-central; FCR: right fronto-central; TL: left temporal; CL: left central; Cz: midline central; CR: right central; TR: right temporal; TPL: left temporo-parietal; CPL: left centro-parietal; CPR: right centro-parietal; TPR: right temporo-parietal; PL: left parietal; PR: right parietal; POL: left parieto-occipital; Pz: midline parietal; POR: right parieto-occipital; O: occipital

We also looked at the ERP responses at these peak time-points between HC and MCI:

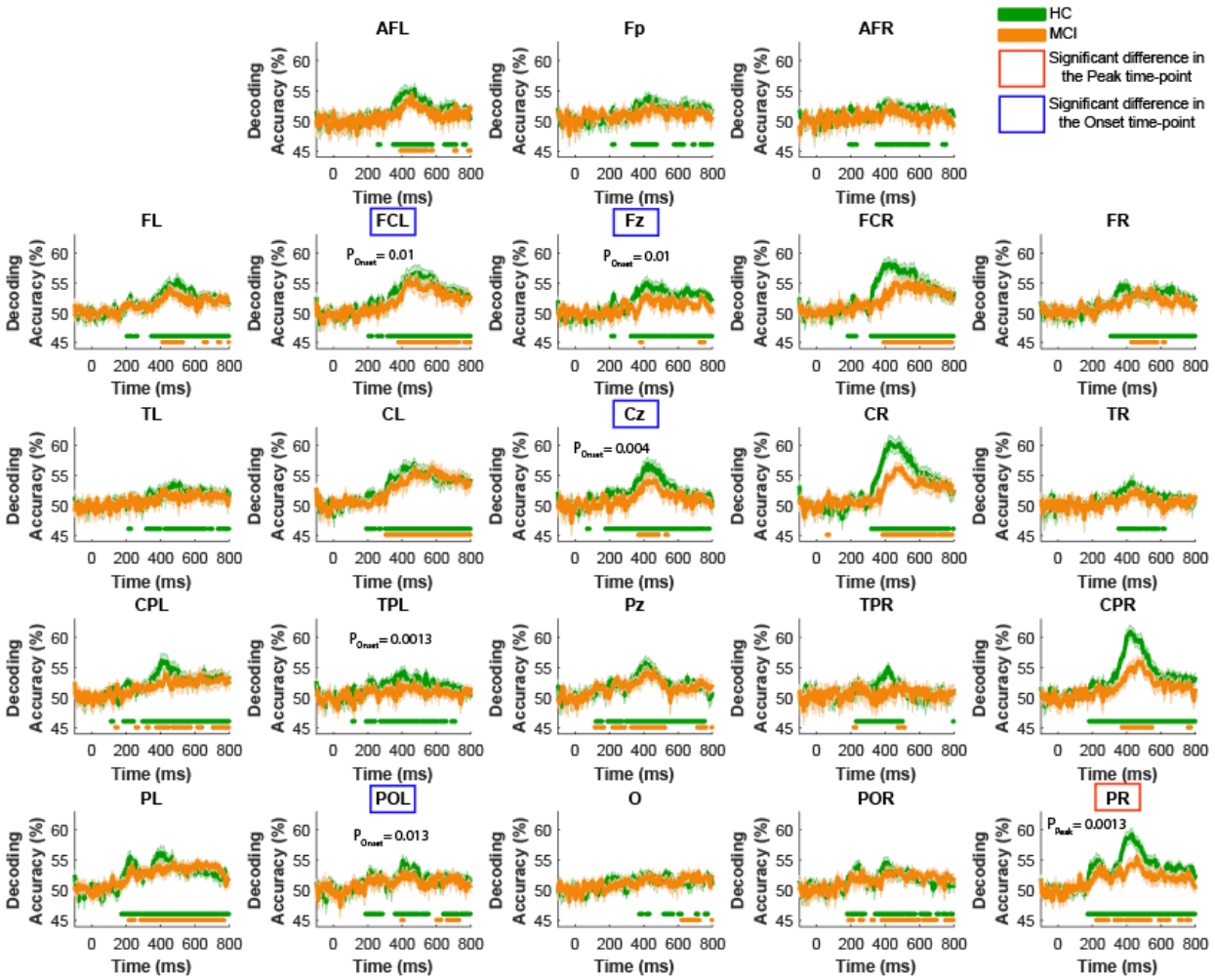

Figure 6. Animal vs. non-animal decoding time course across groups of EEG channels. Horizontal color dots indicate time-points with significant decoding accuracy in the corresponding group (green for HC and orange for MCI). In regions specified with red rectangles MCI's peak animacy decoding time-point is significantly later than that of HC; in regions specified with blue rectangles MCI's onset of animacy decoding significance is significantly later than that of HC (FDR-corrected at 0.05; bootstrap test with 10,000 resampling of participants on MCI minus HC time-points).

channels in the right and left parietals, right temporal-parietal, midline parietal, and midline frontal lobes were significantly activated in both groups. HC showed significant activation levels in the right parieto-occipital, right temporal, and central lobes (midline central, right and left central-parietals, right central, and fronto-central); however, these were absent from the MCI brain activation map. On the other hand, only MCI patients show significant activation on the left parieto-occipital lobe.

Analyzing the behavioral data of participants while taking the ICA test (on an iPad outside the EEG), we find the results are consistent with the findings from the EEG data: the speed and accuracy of animacy detection, as measured by the ICA test, are also significantly deteriorated in patients with MCI (p-value = 0.025 and p-value = 0.037 respectively) (Figures 5f, 5g).

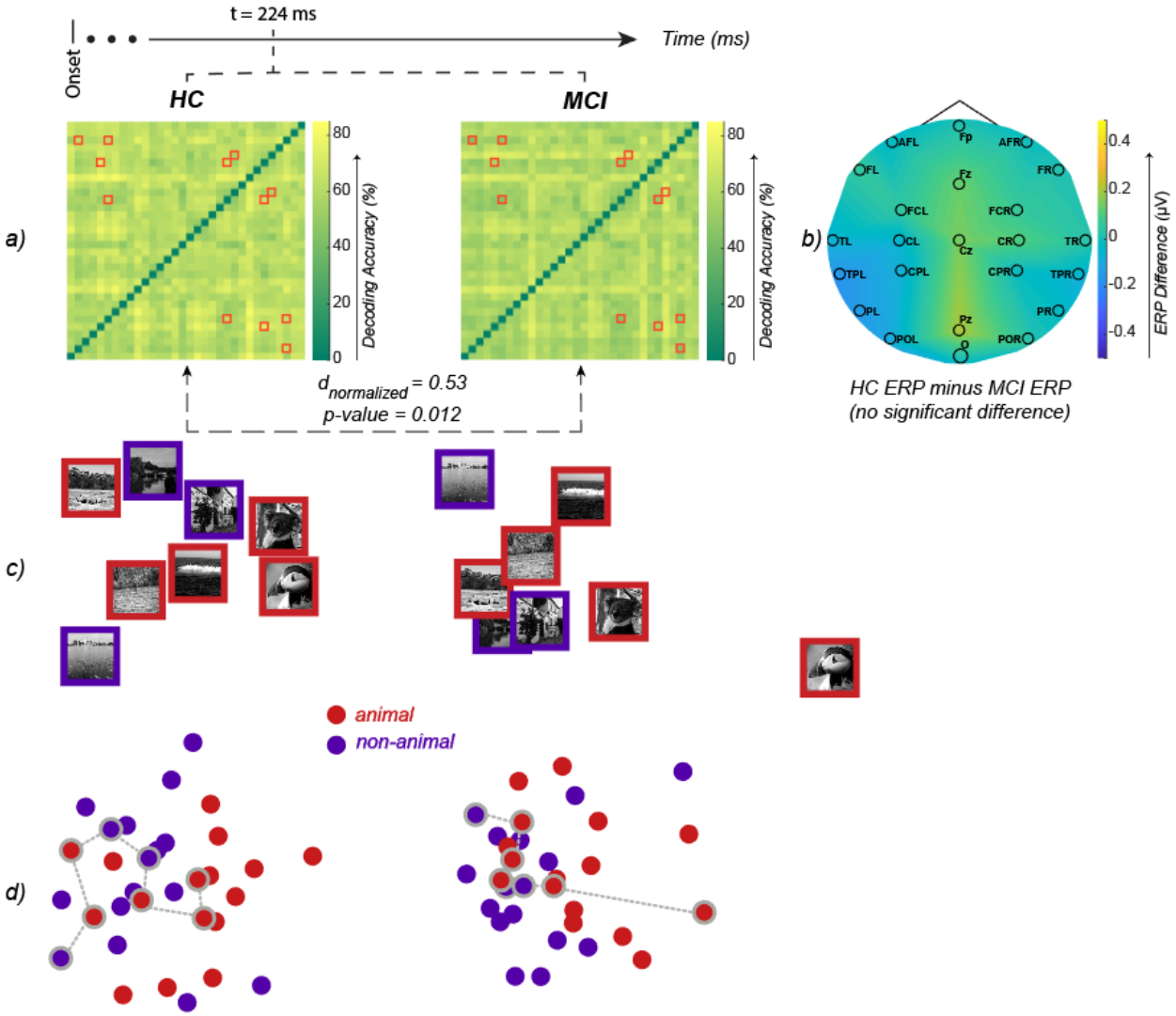

Figure 7. a) The RDM of HC and MCI at the time-point of maximum Euclidean distance (t = 224 ms, d = 146.6, p-value = 0.012, permutation test). We further normalized the Euclidean distance to make it more meaningful by fitting a logarithmic function on the maximum distance (222.7), baseline distance (115.7) and the minimum distance (0). The logarithmic function scales the distances to the [0, 1] interval, and the observed distance between RDMs becomes 0.53. The highlighted elements (i.e. red-squares) of the RDMs are the pairwise dissimilarities with a significant difference between HC and MCI (FDR-corrected at 0.05 rank-sum). b) Difference of the mean ERPs across EEG channels (HC minus MCI) at t=224ms. None of the EEG channels show a significant difference (all p-values > 0.05) between HC and MCI at this time-point. c) MDS of the stimuli that showed a significant difference in their pairwise dissimilarity between HC and MCI (those specified by red squares in the two RDMs). d) MDS of all the stimuli. The dots that are connected with dashed lines are the same stimuli shown in panel 'c'.

We also looked at the channel-specific animacy decoding time courses to investigate whether there is a significant delay in the peak and/or the onset of animacy processing in MCI patients at the level of EEG channels (Figure 6). We found that there is a significant delay in the animacy decoding peak time-point of MCI patients in the right parietal lobe compared to HC (p-value = 0.0013, Figure 6). Additionally, the significance of animal vs.

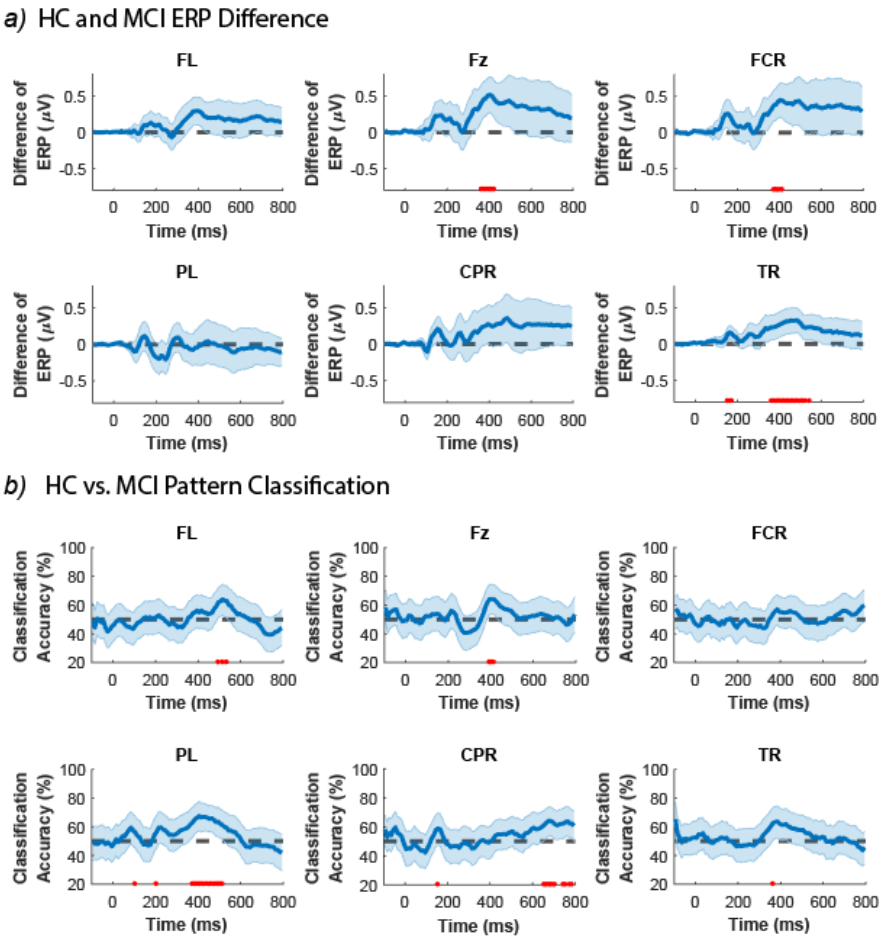

Figure 8. a) HC and. MCI ERP differences in regions where either the ERP difference or the HC vs. MCI classification were statistically significant. The shaded error bars indicate 95% confidence interval of the ERP difference (HC minus MCI). Red dots indicate time-points with significant level of difference in ERP (FDR-corrected at 0.05 across time; rank-sum). b) The HC vs. MCI classification based on the pattern of EEG data (i.e. channels × stimuli), in regions where either the ERP difference or the HC vs. MCI classification of EEG responses were statistically significant. The shaded error bars indicate 95% confidence intervals. Red dots indicate time-points with significant HC vs. MCI classification accuracy (FDR-corrected at 0.05; 10000 bootstrap resampling of subjects).

FL: left frontal; Fz: midline frontal; FCR: right fronto-central; PL: left parietal; CPR: right central parietal; TR: right temporal;

non-animal decoding starts later in the MCI patients in EEG channels of left fronto-central, midline frontal, midline central, and left parieto-occipital lobes (Figure 6).

Comparing Patterns of Visual Information Processing in HC and MCI

We compared patterns of visual information processing in HC and MCI using their RDMs over time. The maximum difference between HC and MCI RDMs was observed at t = 224ms after the stimulus onset (scaled Euclidean distance, d = 0.53 [out of 1], p-value = 0.012; Figure 7a). At this time-point (t=224 ms), an SVM classifier (leave-one-out cross-validation) could significantly discriminate between HC and MCI patterns of visual information (represented by their RDMs) with an accuracy of 70.4% (p-value = 0.0036, 10,000 bootstrap sampling of participants).

We also looked at the univariate differences between HC and MCI at the same time-point (i.e., t = 224 ms); there was no significant difference between the two groups in their ERP responses (Figure 7b). This demonstrates that the response patterns carry valuable information above and beyond what is captured in the neural activity's mean responses.

Furthermore, looking at the HC and MCI RDMs, we highlighted RDM cells that were significantly different between the two groups (Figure 7a). Each RDM cell represents the difference between the EEG patterns of the two stimuli at a given time-point. To provide a more intuitive understating of the differences in patterns, we used multidimensional scaling (MDS) to visualize the RDMs on a 2D surface. Figure 7c illustrates the stimuli with a significant difference between HC and MCI, and Figure 7d visualizes all the stimuli.

Temporal Dynamics of Animacy Categorization

To study the temporal dynamics of animacy categorization in HC and MCI, we compared the mean response (i.e., ERP) as well as EEG activation patterns (i.e., 63 channels × 32 stimuli matrices) between HC and MCI over time. For each EEG channel group, we measured the ERP differences between HC and MCI over time: midline frontal, right fronto-central, and right temporal regions showed a significant difference (Figure 8a). We also performed a classification over the EEG activation patterns to see if HC and MCI can be discriminated based on their epoched EEG responses. HC and MCI could be discriminated based on their EEG activation patterns in the left frontal, midline frontal, left parietal, and right central parietal lobes (Figure 8b).

Looking at the EEG data (Figure 8), we find that HC and MCI can be discriminated starting from 375ms in the left parietal (PL) and from 495ms in the left frontal (FL) both to 515ms after the stimulus onset only based on their patterns of activity, but not the ERPs. Additionally, the pattern of activity in centro-parietal (CPR) can discriminate HC from MCI in almost every time-points after t=655ms. On the other hand, the ERP responses show a significant difference between HC and MCI in the right fronto-central (FCR) at around t=405ms and in the right temporal (TR) from155ms to 174ms and 365ms to 545ms. At the same time-points two groups could not be separated based on their activation patterns. The midline frontal (Fz) was the only region that could differentiate HC and MCI based on both the ERP responses and the activation patterns at around t=405ms after the stimulus onset.

In the previous subsection, we demonstrated that at t=224 ms, the difference between HC and MCI in the EEG response patterns (captured by RDM) was at its maximum, while the level of activity (captured by ERP) remains unchanged. Here, we identified five groups of channels whose EEG data could discriminate between HC and MCI, either based on the activation patterns or the ERP responses, but not both. This is consistent with the reported results in the previous section, demonstrating that EEG activation patterns could be different even though there might be no difference at the level of ERP.

Discussion

In this study, we investigated the temporal dynamics of animacy visual processing in patients with MCI. We argued that the speed of processing animacy information is a potential biomarker for detecting MCI, which is likely to be more sensitive to subtle brain deterioration than memory symptoms.

Previous resting-state and task-based EEG studies have focused on univariate changes (e.g., ERP, frequency bands, connectivity) in patients with MCI and individuals with mild to moderate AD (P. Missonnier et al. 2007; F. J. Fraga et al. 2017; Pijnenburg et al. 2004; Pascal Missonnier et al. 2005; Vecchio et al. 2014; Francisco J. Fraga et al. 2018; Babiloni et al. 2016). Here, using a rapid visual categorization task and applying multivariate pattern analysis, we looked beyond the univariate changes and studied the categorical representation of animacy information in the brain of old healthy individuals and patients with MCI. We demonstrated that patients with MCI could be discriminated from HC based on their pattern of animacy representation. Furthermore, we identified regions in which either the mean EEG responses of the pattern of brain activity show significant differences between HC and MCI.

Task Differences in EEG studies of HC and MCI

Consistent with previous reports in resting-state EEG studies (Babiloni et al. 2006) and studies with a visual memory task (F. J. Fraga et al. 2017), we observed univariate differences between HC and MCI in the temporal and the fronto-central electrodes.

In contrast, we did not find any significant difference in ERP responses of HC vs. MCI in centro-parietal and parietal electrodes –which is reported previously in an EEG study with a visual working memory task (Francisco J. Fraga et al. 2018). We also observed no univariate difference in the frontal and occipital electrodes, while previous resting-state EEG studies have reported differences between HC and MCI in these regions (Choi et al. 2019; Babiloni et al. 2006). On the other hand, we found that MCI patients could be discriminated from HC based on their ERP responses of the midline frontal region electrodes. These differences could potentially be explained by the difference in the tasks used for each of these studies (i.e., visual working memory and resting-state vs. rapid visual categorization).

In addition to the previous univariate findings, here we revealed multivariate differences between HC and MCI in their patterns of EEG responses: midline frontal, left frontal, left parietal and right centro-parietal electrodes showed significant multivariate differences between HC and MCI. Furthermore, the categorical representation of animacy information of the right parietal electrode emerged later in the MCI patients compared to that of HC. Also, in comparison with HC, the MCI patients had significantly longer onset latencies of

animacy information in the left fronto-central, midline frontal, midline central, and left parieto-occipital electrodes.

Neural Speed of Information Processing in MCI patients

Rapid recognition of animate objects is a fundamental ability of human visual cognition. Previous M/EEG studies have investigated the temporal neural dynamics of animacy processing in young healthy individuals. Using slightly different visual tasks and stimuli, studies have shown that the onset and peak of animacy decoding emerges between 66ms to 157ms (Cichy, Pantazis, and Oliva 2014); or from 80ms to 240ms (Carlson et al. 2013) after the stimulus onset. Here, we showed that in old healthy individuals, the onset and the peak of animacy decoding emerges between 131ms (SE=30) and 434ms (SE=30) after the stimulus onset. This result indicates that normal aging causes a reduction in the animacy information processing speed (IPS). Compared to the old healthy individuals, animacy IPS was further delayed in MCI patients (onset of animacy decoding: 196ms ±16, peak animacy decoding: 473ms ±34 after the stimulus onset). These findings confirm a significant decrease in the speed of neural information processing in patients with MCI and are consistent with previous behavioral studies showing a decline in visual IPS in MCI patients compared to HC (Khaligh-Razavi et al. 2019; Ruiz-Rizzo et al. 2017). Together, these results suggest the IPS as a potential biomarker for the early detection of AD, along with memory symptoms or ideally before the onset of memory symptoms.

Acknowledgement

Authors would like to thank the Iranian Cognitive Sciences and Technologies Council (COGC) for the grant awarded to SKR (#4873). We thank the National Brain Mapping Laboratory (NBML), where all the EEG data acquisitions were done. Authors are also grateful to Mohammad Mohaghar for proofreading the manuscript.

References

"2018 Alzheimer's Disease Facts and Figures." 2018. *Alzheimer's & Dementia: The Journal of the Alzheimer's Association* 14 (3): 367–429. https://doi.org/10.1016/j.jalz.2018.02.001.

Babiloni, Claudio, Roberta Lizio, Nicola Marzano, Paolo Capotosto, Andrea Soricelli, Antonio Ivano Triggiani, Susanna Cordone, Loreto Gesualdo, and Claudio Del Percio.

2016. "Brain Neural Synchronization and Functional Coupling in Alzheimer's Disease as Revealed by Resting State EEG Rhythms." *International Journal of Psychophysiology*, Research on Brain Oscillations and Connectivity in A New Take-Off State, 103 (May): 88–102. https://doi.org/10.1016/j.ijpsycho.2015.02.008.

Bacon-Macé, Nadège, Marc J. -M. Macé, Michèle Fabre-Thorpe, and Simon J. Thorpe. 2005. "The Time Course of Visual Processing: Backward Masking and Natural Scene Categorisation." *Vision Research* 45 (11): 1459–69. https://doi.org/10.1016/j.visres.2005.01.004.

Bell, Mary A., and Melvyn J. Ball. 1990. "Neuritic Plaques and Vessels of Visual Cortex in Aging and Alzheimer's Dementia." *Neurobiology of Aging* 11 (4): 359–70. https://doi.org/10.1016/0197-4580(90)90001-G.

Carlson, Thomas, David A. Tovar, Arjen Alink, and Nikolaus Kriegeskorte. 2013. "Representational Dynamics of Object Vision: The First 1000 Ms." *Journal of Vision* 13 (10): 1–1. https://doi.org/10.1167/13.10.1.

Cichy, Radoslaw Martin, Dimitrios Pantazis, and Aude Oliva. 2014. "Resolving Human Object Recognition in Space and Time." *Nature Neuroscience* 17 (3): 455–62. https://doi.org/10.1038/nn.3635.

Cogan, D. G. 1979. "Visuospatial Dysgnosia." *American Journal of Ophthalmology* 88 (3 Pt 1): 361–68. https://doi.org/10.1016/0002-9394(79)90634-2.

Cogan, David G. 1985. "Visual Disturbances With Focal Progressive Dementing Disease." *American Journal of Ophthalmology* 100 (1): 68–72. https://doi.org/10.1016/S0002-9394(14)74985-2.

Connolly, Andrew C., J. Swaroop Guntupalli, Jason Gors, Michael Hanke, Yaroslav O. Halchenko, Yu-Chien Wu, Hervé Abdi, and James V. Haxby. 2012. "The Representation of Biological Classes in the Human Brain." *Journal of Neuroscience* 32 (8): 2608–18. https://doi.org/10.1523/JNEUROSCI.5547-11.2012.

Deursen, J. A. van, E. F. P. M. Vuurman, F. R. J. Verhey, V. H. J. M. van Kranen-Mastenbroek, and W. J. Riedel. 2008. "Increased EEG Gamma Band Activity in Alzheimer's Disease and Mild Cognitive Impairment." *Journal of Neural Transmission* 115 (9): 1301–11. https://doi.org/10.1007/s00702-008-0083-y.

Fraga, F. J., L. A. Ferreira, T. H. Falk, E. Johns, and N. D. Phillips. 2017. "Event-Related Synchronisation Responses to N-Back Memory Tasks Discriminate between Healthy Ageing, Mild Cognitive Impairment, and Mild Alzheimer's Disease." In *2017 IEEE International Conference on Acoustics, Speech and Signal Processing (ICASSP)*, 964–68. https://doi.org/10.1109/ICASSP.2017.7952299.

Fraga, Francisco J., Godofredo Quispe Mamani, Erin Johns, Guilherme Tavares, Tiago H. Falk, and Natalie A. Phillips. 2018. "Early Diagnosis of Mild Cognitive Impairment and Alzheimer's with Event-Related Potentials and Event-Related Desynchronization in N-Back Working Memory Tasks." *Computer Methods and Programs in Biomedicine* 164 (October): 1–13. https://doi.org/10.1016/j.cmpb.2018.06.011.

Han, Yuliang, Kai Wang, Jianjun Jia, and Weiping Wu. 2017. "Changes of EEG Spectra and Functional Connectivity during an Object-Location Memory Task in Alzheimer's Disease." *Frontiers in Behavioral Neuroscience* 11 (May). https://doi.org/10.3389/fnbeh.2017.00107.

Holroyd, Suzanne, and Michael L. Shepherd. 2001. "Alzheimer's Disease: A Review for the Ophthalmologist." *Survey of Ophthalmology* 45 (6): 516–24. https://doi.org/10.1016/S0039-6257(01)00193-X.

Iseri, Pervin, Özgül Altinaş, Tomris Tokay, and Nurşen Yüksel. 2006. "Relationship between Cognitive Impairment and Retinal Morphological and Visual Functional Abnormalities in Alzheimer Disease." *Journal of Neuro-Ophthalmology* 26 (1): 18–24. https://doi.org/10.1097/01.wno.0000204645.56873.26.

Jackson, Gregory R, and Cynthia Owsley. 2003. "Visual Dysfunction, Neurodegenerative Diseases, and Aging." *Neurologic Clinics* 21 (3): 709–28. https://doi.org/10.1016/S0733-8619(02)00107-X.

Katz, Barrett, and Steve Rimmer. 1989. "Ophthalmologic Manifestations of Alzheimer's Disease." *Survey of Ophthalmology* 34 (1): 31–43. https://doi.org/10.1016/0039-6257(89)90127-6.

Khaligh-Razavi, Seyed-Mahdi, Sina Habibi, Maryam Sadeghi, Haniye Marefat, Mahdiyeh Khanbagi, Seyed Massood Nabavi, Elham Sadeghi, and Chris Kalafatis. 2019. "Integrated Cognitive Assessment: Speed and Accuracy of Visual Processing as a Reliable Proxy to Cognitive Performance." *Scientific Reports* 9 (January). https://doi.org/10.1038/s41598-018-37709-x.

Khaligh-Razavi, Seyed-Mahdi, and Nikolaus Kriegeskorte. 2014. "Deep Supervised, but Not Unsupervised, Models May Explain IT Cortical Representation." *PLOS Computational Biology* 10 (11): e1003915. https://doi.org/10.1371/journal.pcbi.1003915.

Kiani, Roozbeh, Hossein Esteky, Koorosh Mirpour, and Keiji Tanaka. 2007. "Object Category Structure in Response Patterns of Neuronal Population in Monkey Inferior Temporal Cortex." *Journal of Neurophysiology* 97 (6): 4296–4309. https://doi.org/10.1152/jn.00024.2007.

Kriegeskorte, Nikolaus, Marieke Mur, Douglas A. Ruff, Roozbeh Kiani, Jerzy Bodurka, Hossein Esteky, Keiji Tanaka, and Peter A. Bandettini. 2008. “Matching Categorical Object Representations in Inferior Temporal Cortex of Man and Monkey.” *Neuron* 60 (6): 1126–41. https://doi.org/10.1016/j.neuron.2008.10.043.

Mendez, M. F., R. L. Tomsak, and B. Remler. 1990. “Disorders of the Visual System in Alzheimer’s Disease.” *Journal of Clinical Neuro-Ophthalmology* 10 (1): 62–69.

Missonnier, P., M.-P. Deiber, G. Gold, F. R. Herrmann, P. Millet, A. Michon, L. Fazio-Costa, V. Ibañez, and P. Giannakopoulos. 2007. “Working Memory Load-Related Electroencephalographic Parameters Can Differentiate Progressive from Stable Mild Cognitive Impairment.” *Neuroscience* 150 (2): 346–56. https://doi.org/10.1016/j.neuroscience.2007.09.009.

Pijnenburg, Y. a. L., Y. v d Made, A. M. van Cappellen van Walsum, D. L. Knol, Ph Scheltens, and C. J. Stam. 2004. “EEG Synchronization Likelihood in Mild Cognitive Impairment and Alzheimer’s Disease during a Working Memory Task.” *Clinical Neurophysiology: Official Journal of the International Federation of Clinical Neurophysiology* 115 (6): 1332–39. https://doi.org/10.1016/j.clinph.2003.12.029.

Sadun, Alfredo A., Mark Borchert, Edward DeVita, David R. Hinton, and Carl J. Bassi. 1987. “Assessment of Visual Impairment in Patients With Alzheimer’s Disease.” *American Journal of Ophthalmology* 104 (2): 113–20. https://doi.org/10.1016/0002-9394(87)90001-8.

Thorpe, Simon J. 2009. “The Speed of Categorization in the Human Visual System.” *Neuron* 62 (2): 168–70. https://doi.org/10.1016/j.neuron.2009.04.012.

Vecchio, Fabrizio, Francesca Miraglia, Camillo Marra, Davide Quaranta, Maria Gabriella Vita, Placido Bramanti, and Paolo Maria Rossini. 2014. “Human Brain Networks in Cognitive Decline: A Graph Theoretical Analysis of Cortical Connectivity from EEG Data.” *Journal of Alzheimer’s Disease: JAD* 41 (1): 113–27. https://doi.org/10.3233/JAD-132087.

Ward, Alex, Sarah Tardiff, Catherine Dye, and H. Michael Arrighi. 2013. “Rate of Conversion from Prodromal Alzheimer’s Disease to Alzheimer’s Dementia: A Systematic Review of the Literature.” *Dementia and Geriatric Cognitive Disorders Extra* 3 (1): 320–32. https://doi.org/10.1159/000354370.